Supplementary information

Enhanced norfloxacin removal by eco-friendly $MgFe_2O_4$ modified sugarcane bagasse biochar: Adsorption performances and mechanisms

Yan He*, Tong Liu, Yuehua Deng

College of Geology and Environment, Xi'an University of Science and Technology, Xi'an 710054, China.

*Corresponding Author: nkheyan@163.com (Yan He)

Test S1. The equations and parameters of adsorption kinetic, isotherm and thermodynamic models.

Pseudo-first-order (Eq. (1)), pseudo-second-order (Eq. (2)) and intra-particle diffusion (Eq. (3)) models were used to fit the kinetic data. Langmuir (Eq. (4) and Eq. (5)), Freundlich (Eq. (6)), Temkin (Eq. (7)) and Dubinin-Radushkevich isotherm models (Eq. (8), Eq. (9) and Eq. (10)) were applied to fit the isothermal data. The thermodynamic parameters were calculated by the following Eq. (11) and Eq. (12).

$$Q_t = Q_e(1 - e^{-k_1 t}) \quad (1)$$

$$Q_t = \frac{Q_e^2 k_2 t}{1 + Q_e k_2 t} \quad (2)$$

$$Q_t = k_i t^{1/2} + C_i \quad (3)$$

$$Q_e = \frac{Q_m K_L C_e}{1 + K_L C_e} \quad (4)$$

$$RL = \frac{1}{1 + KLC0} \quad (5)$$

$$Q_e = K_F C_e^{1/n} \quad (6)$$

$$Q_e = \frac{RT}{B_T} \ln(K_T C_e) \quad (7)$$

$$Q_e = Q_m e^{-K_D \varepsilon^2} \quad (8)$$

$$\varepsilon = RT\ln(1 + 1/C_e) \quad (9)$$

$$E = (2K_D)^{-0.5} \quad (10)$$

$$\Delta G^0 = \Delta H^0 - T\Delta S^0 \quad (11)$$

$$\ln\frac{Q_e}{C_e} = \frac{\Delta S^0}{R} - \frac{\Delta H^0}{RT} \quad (12)$$

where Q_t (mg/g) and Q_e(mg/g) are the adsorption amount at time t (min) and equilibrium, respectively; k_1 (1/min), k_2 (g/(mg·min)) and ki (mg/g·$min^{1/2}$) represent the rate constants of pseudo-first-order, pseudo-second-order and intraparticle diffusion models, respectively; C_i (mg/g) is related to the thickness of the boundary layer; C_e (mg/L) is the adsorption equilibrium concentration; Q_m (mg/g) is the maximum adsorption capacity; K_L (L/mg) is the Langmuir equilibrium constant;

R_L is dimensionless separation factor; K_F (mg/g·(L/mg)$^{1/n}$) is the Freundlich equilibrium constant and represents the adsorption capacity; n is the isothermal constant and represents the adsorption strength; R is the gas constant (8.314 J/mol·K); T (K) is the absolute temperature; B_T (kJ/mol) is the Temkin constant related to the heat of sorption; and K_T (L/mg) is the Temkin binding constant; K_D (mol^2/J^2) is the constant related to adsorption energy; ε is the Polanyi potential; E (kJ/mol) is the adsorption free energy; ΔG^0 (kJ/ mol), ΔH^0 (kJ/mol) and ΔS^0 (kJ/(mol·K)) are the changes in Gibbs free energy, enthalpy and entropy, respectively.

Test S2. The calculation process of ionization distribution of NOR.

$$NOR^{+}(\%) = \frac{(10^{(-pH)})^2}{(10^{(-pH)})^2 + 10^{(-pK_{a1})} \times 10^{(-pH)} + 10^{(-pK_{a1})} \times 10^{(-pK_{a2})}} \times 100 \quad (13)$$

$$NOR^{\pm}(\%) = \frac{10^{(-pk_{a1})} \times 10^{(-pH)}}{(10^{(-pH)})^2 + 10^{(-pK_{a1})} \times 10^{(-pH)} + 10^{(-pK_{a1})} \times 10^{(-pK_{a2})}} \times 100 \quad (14)$$

$$NOR^{-}(\%) = \frac{10^{(-pk_{a1})} \times 10^{(-pk_{a2})}}{(10^{(-pH)})^2 + 10^{(-pK_{a1})} \times 10^{(-pH)} + 10^{(-pK_{a1})} \times 10^{(-pK_{a2})}} \times 100 \quad (15)$$

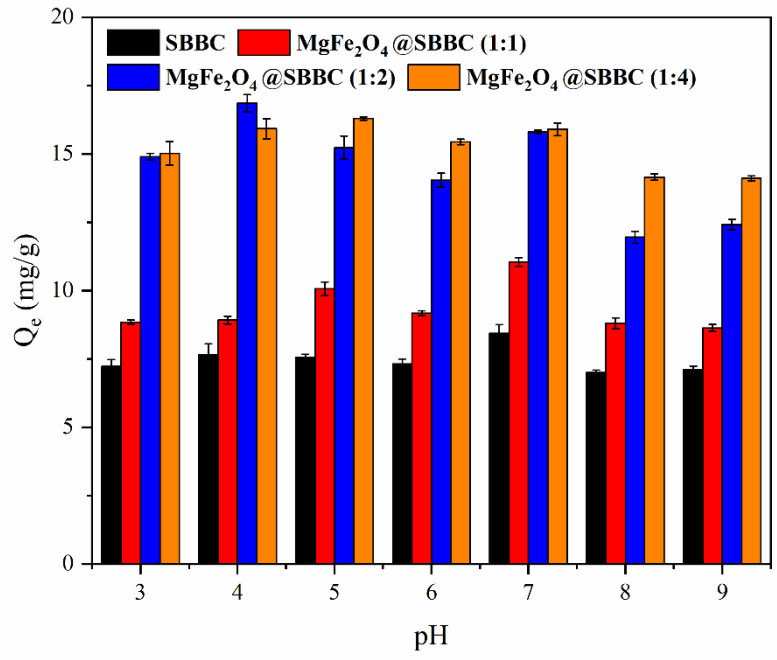

Fig. S1. NOR adsorption capacities of different biochar materials.

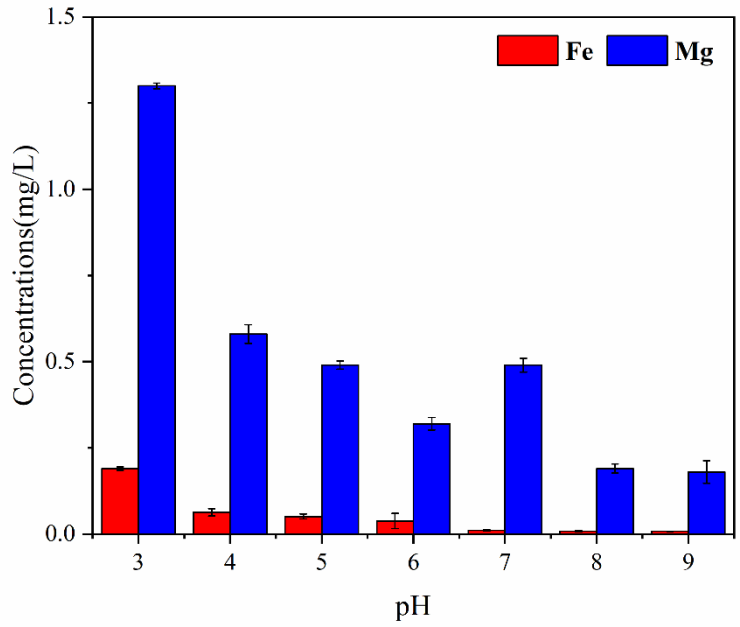

Fig. S2. Metal leaching concentrations at different pH conditions.

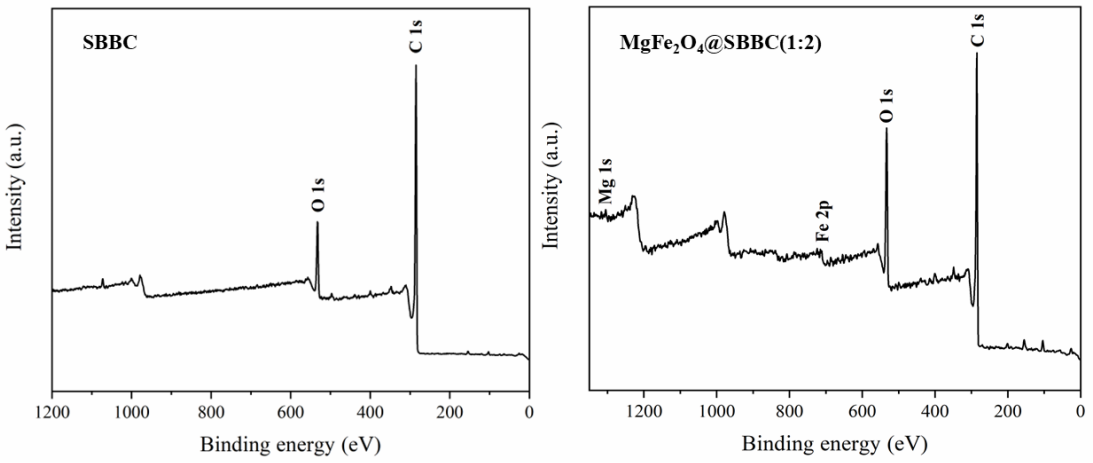

Fig. S3. XPS survey spectra of SBBC and $MgFe_2O_4$@SBBC(1:2).

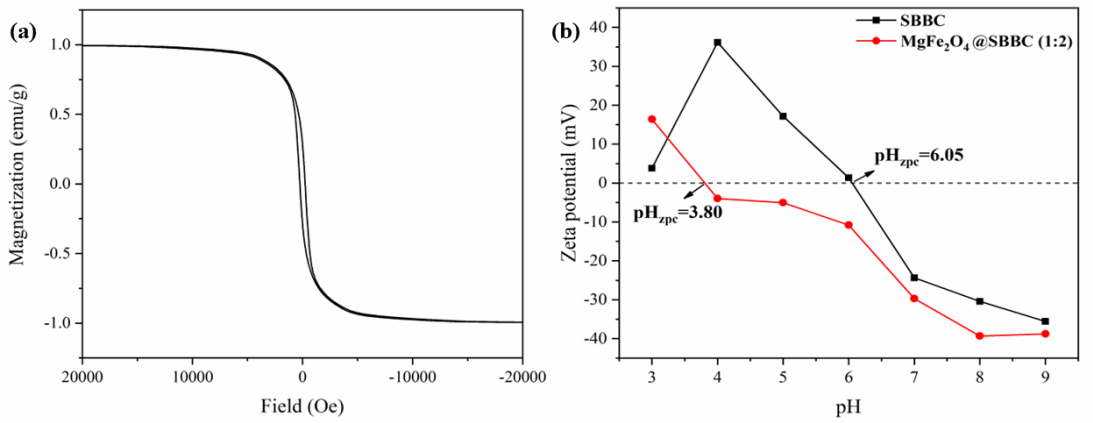

Fig. S4. Magnetic hysteresis curve of $MgFe_2O_4$@SBBC(1:2) (a) and zeta potentials of SBBC and $MgFe_2O_4$@SBBC(1:2) (b).

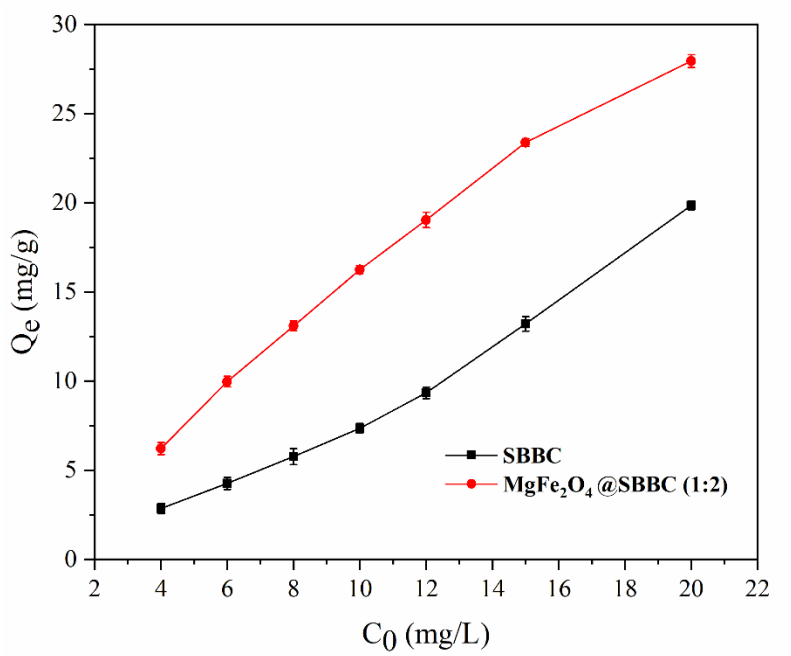

Fig. S5. Effect of initial concentrations on the NOR adsorption onto SBBC and $MgFe_2O_4$@SBBC(1:2).

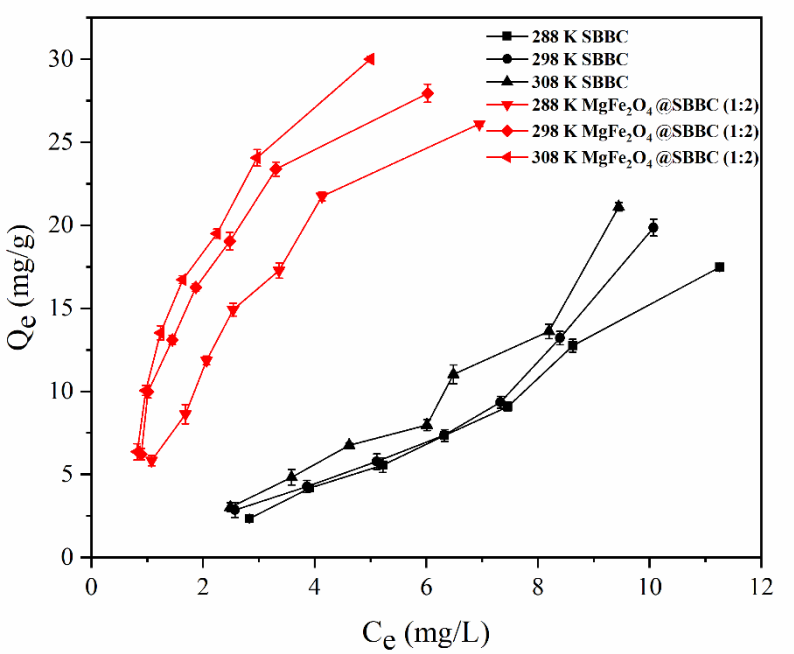

Fig. S6. Effect of temperature on the NOR adsorption onto SBBC and $MgFe_2O_4$@SBBC(1:2).

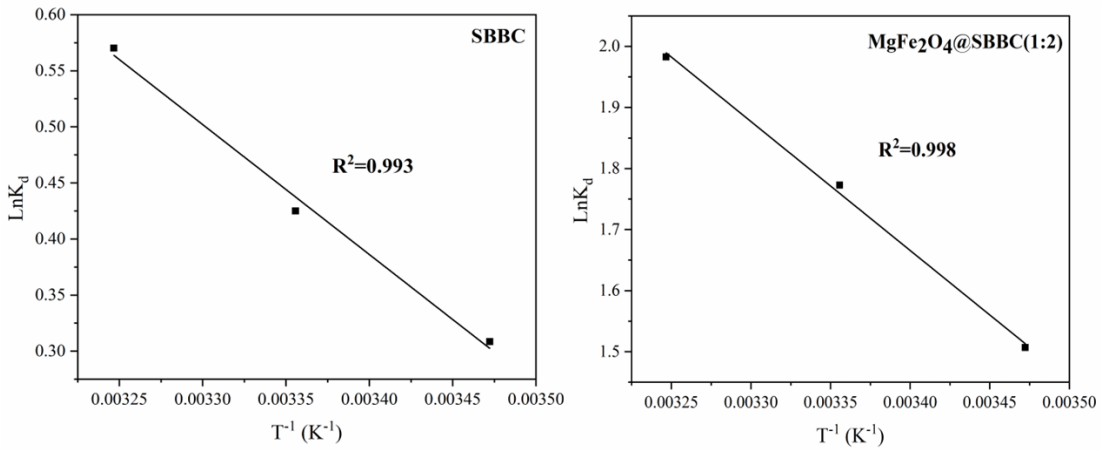

Fig. S7. Thermodynamic studies of NOR adsorption on SBBC and $MgFe_2O_4$@SBBC(1:2).

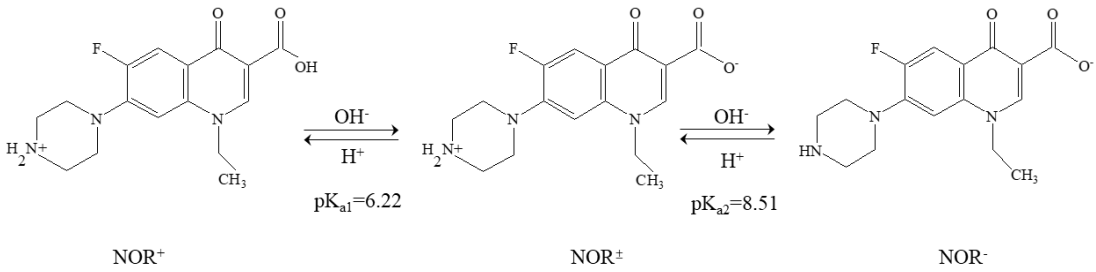

Fig. S8. Chemical speciation of NOR in aqueous solution.

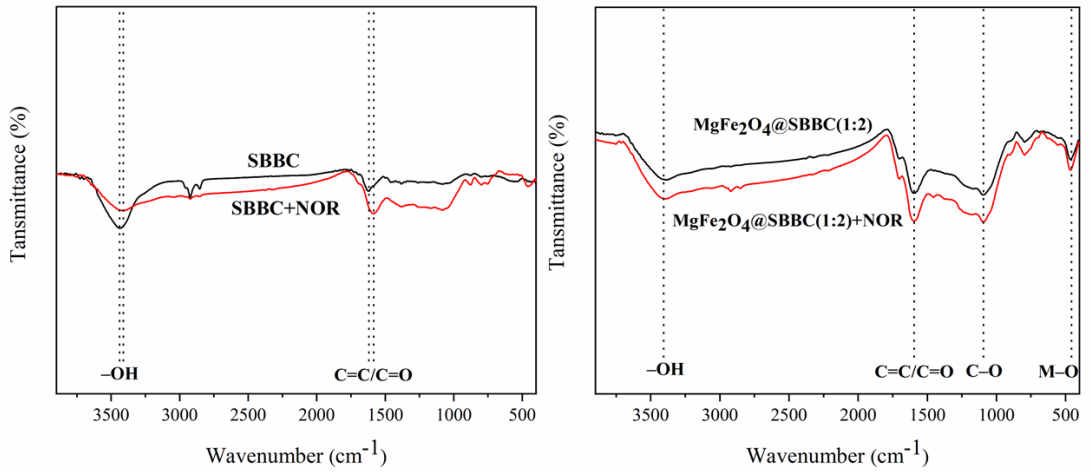

Fig. S9. FTIR spectra of SBBC and $MgFe_2O_4$@SBBC(1:2) before and after adsorption.

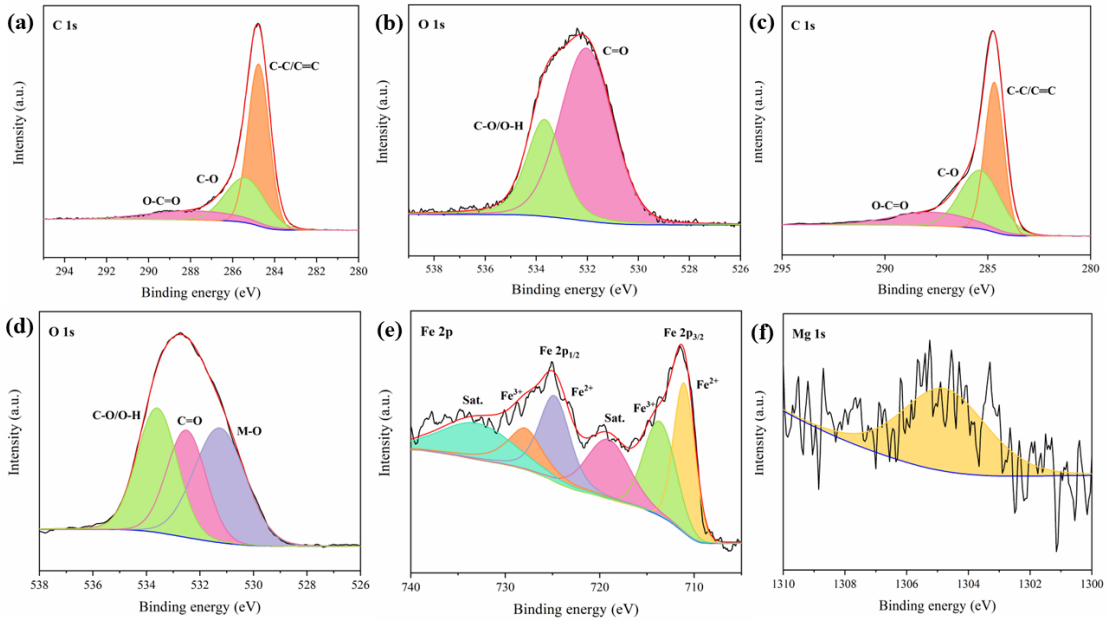

Fig. S10. XPS spectra C 1s and O 1s of SBBC (a, b) and C 1s, O 1s, Fe 2p and Mg 1s of $MgFe_2O_4$@SBBC(1:2) (c–f) after adsorption.

Table S1. S_{BET}, V_p, and D_p values of SBBC and $MgFe_2O_4$@SBBC(1:2) after adsorption.

Sample	S_{BET} (m^2/g)	V_p (cm^3/g)	D_p (nm)
SBBC+NOR	90	0.09	3.98
$MgFe_2O_4$@SBBC(1:2)+NOR	196	0.14	2.76

Table S2. Summary of the peak area ratio of C 1s and O 1s of SBBC before and after adsorption.

Binding energy (eV)	284.6	285.8	288.5
Functional groups	C–C/C=C (%)	C–O (%)	O–C=O (%)
SBBC	60.8	25.3	13.9
SBBC+NOR	56.5	29.6	13.9

Binding energy (eV)	532.0	533.6
Functional groups	C–O (%)	O–C=O (%)
SBBC	64.0	36.0
SBBC+NOR	70.0	30.0

Table S3. Summary of the peak area ratio of C 1s, O 1s, and Fe 2p of $MgFe_2O_4$@SBBC(1:2) before and after adsorption.

Binding energy (eV)	284.6	285.8	288.5
Functional groups	C–C/C=C (%)	C–O (%)	O–C=O (%)
$MgFe_2O_4$@SBBC(1:2)	62.8	19.9	17.3
$MgFe_2O_4$@SBBC(1:2)+NOR	45.1	36.8	18.1

Binding energy (eV)	531.3	532.5	533.6

Functional groups	M–O (%)	C=O (%)	C–O/O–H (%)
$MgFe_2O_4$@SBBC(1:2)	36.9	36.1	27.0
$MgFe_2O_4$@SBBC(1:2)+NOR	38.7	27.5	33.8

83

Binding energy (eV)	711.4, 724.5	713.5, 726.0
Valence state	Fe^{2+} (%)	Fe^{3+} (%)
$MgFe_2O_4$@SBBC(1:2)	45.5	26.3
$MgFe_2O_4$@SBBC(1:2)+NOR	33.6	29.4

84